

Tuning the optical emission of MoS₂ nanosheets using proximal photoswitchable azobenzene molecules

Juan Li, Jakob Wierzbowski, Özlem Ceylan, Julian Klein, Filippo Nisic, Tuan Le Anh, Felix Meggendorfer, Carlos-Andres Palma, Claudia Dragonetti, Johannes V. Barth, Jonathan J. Finley, and Emanuela Margapoti

Citation: *Applied Physics Letters* **105**, 241116 (2014); doi: 10.1063/1.4904824

View online: <http://dx.doi.org/10.1063/1.4904824>

View Table of Contents: <http://scitation.aip.org/content/aip/journal/apl/105/24?ver=pdfcov>

Published by the [AIP Publishing](#)

Articles you may be interested in

[Contact-dependent performance variability of monolayer MoS₂ field-effect transistors](#)

Appl. Phys. Lett. **105**, 213508 (2014); 10.1063/1.4902866

[Reconfigurable p-n junction diodes and the photovoltaic effect in exfoliated MoS₂ films](#)

Appl. Phys. Lett. **104**, 122104 (2014); 10.1063/1.4870067

[Functionalization, self-assembly, and photoswitching quenching for azobenzene derivatives adsorbed on Au\(111\)](#)

J. Chem. Phys. **133**, 234707 (2010); 10.1063/1.3519557

[Reversible work function changes induced by photoisomerization of asymmetric azobenzene dithiol self-assembled monolayers on gold](#)

Appl. Phys. Lett. **93**, 083109 (2008); 10.1063/1.2969468

[Monolayer alignment on azobenzene surfaces during UV light irradiation: Analysis of optical polarized absorption measurement results and theoretical treatment](#)

J. Chem. Phys. **124**, 024701 (2006); 10.1063/1.2141956

An advertisement for Keysight B2980A Series Picoammeters/Electrometers. The ad features a red and white border with a ruler-like scale at the top. The text reads: 'Confidently measure down to 0.01 fA and up to 10 PΩ'. Below this, it says 'Keysight B2980A Series Picoammeters/Electrometers'. To the right is an image of the device, a small, handheld electronic instrument with a screen and buttons. The Keysight Technologies logo is in the bottom right corner. A red button with white text says 'View video demo >'.

Confidently measure down to 0.01 fA and up to 10 PΩ
Keysight B2980A Series Picoammeters/Electrometers
View video demo >
KEYSIGHT TECHNOLOGIES

Tuning the optical emission of MoS₂ nanosheets using proximal photoswitchable azobenzene molecules

Juan Li,^{1,2} Jakob Wierzbowski,¹ Özlem Ceylan,¹ Julian Klein,¹ Filippo Nisic,³ Tuan Le Anh,¹ Felix Megendorfer,¹ Carlos-Andres Palma,² Claudia Dragonetti,³ Johannes V. Barth,² Jonathan J. Finley,¹ and Emanuela Margapoti^{1,a)}

¹Physik Department and NIM, Walter Schottky Institute, Technische Universität München, Am Coulombwall 4, Garching D-85748, Germany

²Physik Department E20, Technische Universität München, James-Franck-St. 1, Garching D-85748, Germany

³Dipartimento di Chimica, Università degli Studi di Milano and UdR dell'INSTM di Milano, Via Golgi 19, I-20133 Milano, Italy

(Received 20 October 2014; accepted 8 December 2014; published online 19 December 2014)

We report photoluminescence measurements performed on monolayer- and two-layer-MoS₂ placed on two types of mixed self-assembled monolayers (mSAMs) of photoswitchable azobenzene molecules. The two mSAMs differ via the electronegative character of the azobenzene derivatives. Thin layers of a transition metal dichalcogenide—MoS₂—were mechanically exfoliated on mSAM to allow for direct interaction between the molecules and the MoS₂ layers. When the MoS₂ nanosheet is in contact with the electropositive azobenzene molecules in *trans* configuration, an emission side band at lower energies and at low excitation powers suggest n-type doping. The photoisomerization of the molecules from *trans* to *cis* configuration lowers the doping, quenching the side band and enhancing the overall PL efficiency by a factor of ~3. Opposite results were observed with the chlorinated, more electronegative molecules, exhibiting a reversed trend in the PL efficiency between *trans* and *cis*, but with an overall larger intensity. The type of doping induced by the two types of mSAMs was determined by Kelvin probe force microscopy technique.

© 2014 AIP Publishing LLC. [<http://dx.doi.org/10.1063/1.4904824>]

Monolayer (1L)-MoS₂^{1,2} is a two-dimensional (2D) material that has attracted considerable attention due to its semiconducting properties including band gap modulation,³ competitive mobility, and large field effect on/off ratios⁴ exceeding 10⁸. These properties make MoS₂ a promising material for developing the next generation of few atom-thin logic devices, photodetectors,⁵ and light emitting diodes.^{6,7}

When scaling down the number of atomic layers to one monolayer of MoS₂, a transition from indirect to direct energy gap occurs, enhancing the efficiency of the photoluminescence (PL) emission at visible wavelengths. Furthermore, due to the strong Coulomb interaction between the electron and hole pair, a stable PL can be measured at room temperature.⁷⁻⁹ Several approaches have been proposed to tune the optical properties of MoS₂. Recently, it has been predicted that straining MoS₂ modifies the size of the bandgap and the carrier effective masses.⁸ Alternatively, the PL intensity can be tuned via electrical gating.⁷ Knowing that the uncontrolled and undesired point defects are formed in the MoS₂ monolayer,^{10,11} we understand that in order to improve the quantum yield of this material, these point defects need to be neutralized. This was already demonstrated by Mouri *et al.*¹² while measuring the PL intensity of 1L-MoS₂, which was drastically enhanced (reduced) when p(n)-type dopants cover its surface. The ability to modulate optical properties by means of external stimuli is highly sought for the design of displays and smart metamaterials.¹³ In this regard, optical tuning of devices represents a technological goal that can be achieved using

photochromic compounds providing a straightforward way to realize photoswitchable devices.¹⁴⁻¹⁶ For instance, chemisorbed, highly ordered azobenzene self-assembled monolayers (SAMs) are widely known to photoisomerize between *trans* and *cis* conformations.^{17,18}

Among various tunable properties of SAMs, which serve as the basis for sensors,¹⁹ memory devices,^{17,20} and organic thin-film transistors,²¹ the quantum efficiency of a semiconductor in intimate contact can also be tuned. Therefore, heterostructures made by sandwiching SAMs between a metallic film and a monolayer of a 2D crystal are expected not only to tune the electronic properties of the 2D materials, as demonstrated previously by Margapoti *et al.*,²² but also to optically modulate their spectroscopic properties. Therefore, keeping in mind that the optoelectronic properties of MoS₂ are influenced by substrate,^{23,24} it is expected that the use of photochromic molecules as electron donors/acceptors should result in the photo-tuning and -switching of the MoS₂ optical properties. In this work, we report photoswitchable optical properties of 1L- and two-layer (2L)-MoS₂ and the tunability of the MoS₂ optical properties by means of a proximal mixed self-assembled monolayers (mSAMs) of photochromic azobenzene molecules. We demonstrate that the proximal SAM facilitates optically gateable doping of the MoS₂ monolayer and gives rise to PL enhancement for p-type doping or quenching for n-type doping.

The enhancement for p-type doping can be explained as the suppression of extra negative charges from negative trions, enhancing the PL recombination of the neutral exciton. In contrast, the n-type doping increases the injection of additional electrons, resulting in a decreasing of the neutral

^{a)}Author to whom correspondence should be addressed. Electronic mail: emanuela.margapoti@wsi.tum.de

exciton peak. This can be understood considering a three level model. The trion ($I_x^{-(+)}$) to neutral (I_x) PL-intensity-ratio can be written as $I_x^{-(+)} / I_x = \gamma_t k_t / \gamma_x \Gamma_t$, where $\gamma_{x(t)}$ is the neutral exciton (trion) radiative decay rate, Γ_t is the trion decay rate, and k_t is the trion formation decay.¹² Therefore, increasing the trion intensity $I_x^{-(+)}$ increases the population of the intermediate trion level through k_t with the consequent lowering of the radiative exciton decay rate γ_x . Moreover, we report on the tunability and reversibility of this effect simply by switching the azobenzene molecules from *trans* to *cis*, which can shift the Fermi level of the system.

We describe the PL effect and Kelvin probe force microscopy (KPFM) on a 1L-MoS₂ and multilayers when directly exfoliated on mSAM. A solid-state laser diode (532 nm) was used for the PL measurements focused to $\sim 0.8 \mu\text{m}^2$ using a Mitutoyo Apo Plan SL objective (NA = 0.55). The maximum excitation power used was maintained below 1190 W/mm² to avoid damaging the MoS₂ flake and mSAM. The PL signal was detected using a liquid-nitrogen-cooled CCD camera via a 0.55 m monochromator. The sample was cooled to ~ 10 K using a cold finger cryostat. The KPFM characterization were performed using an Asylum Research scanning probe microscope employing a Pt-Ir coated Si cantilever with a spring constant of ~ 2 N/m. The KPFM measurements were conducted in a non-contact mode, and the tip was scanned above the sample at a height of 10 nm with a drive frequency of 67 kHz and AC voltage amplitude of 3 V.

The mixed SAMs (mSAM) consist of the well-known^{22,25} photoisomerizable azobenzene derivative (E)-6-(4-(phenyldiazenyl)phenoxy)hexane-1-thiol (HS-C₆AZO) mixed with spacer-molecules, 6-(2-mercapto)-1-hexanol, in the ratio 1:1, such as to prevent aggregation of the photomediated molecular conformational switching.²⁵ Spacer molecules and HS-C₆AZO were purchased from Sigma-Aldrich and Prochimia Surfaces Sp., respectively. The HS-C₆AZO is considered to be electropositive whereas the use of (E)-6-(4-(4-chlorophenyldiazenyl)phenoxy)hexane-1-thiol (HS-C₆AZO-Cl) also mixed with the -(2-mercapto)-1-hexanol in the ratio 1:1 should lead to an electronegative behaviour. The HS-C₆AZO-Cl was synthesized as reported in literature.^{26,27} The mSAM in this case is defined as mSAM-Cl.

MoS₂ flakes (left most panels in Fig. 1(b)) were mechanically exfoliated from bulk crystals onto the functionalised Au-quartz substrate. A scheme of the configuration is shown in Fig. 1(a). Photoisomerization experiments were performed by irradiating the sample with 366 nm UV-laser for 60 min inducing conformational isomerization from *trans* to *cis*. The switching back of the azobenzene molecules from *cis* to *trans* was reached irradiating the sample with a 475 nm laser for 60 min. Typical integrated PL map intensity modulation between *trans* and *cis* of 2L-MoS₂-mSAM is shown in Fig. 1(b). Here, the weak PL intensity (second left image) for the HS-C₆AZO in *trans* can be optically tuned by irradiating the sample with the UV-light. The consecutive panels were recorded at different illumination times up to 60 min, after which the PL map intensity is now much brighter and the azobenzene molecules should be completely switched in *cis*. The switching back of the molecules to *trans* is shown in the last panel. The integrated PL spectra for the exposure time, $t = 0$, before UV-light exposure (red spectrum), after 60 min of UV-light exposure (blue spectrum), and after 60 min of exposure with 475 nm laser (orange spectrum) are shown in Fig. 1(c).

The spectra show a clear enhancement of the intensity of the PL intensity by a factor of three times, switching the HS-C₆AZO from *trans* to *cis*, and results show that the process is reversible. It is worth to mention that during the recording time of the spectra (30 s), the 532 nm wavelength of the excitation laser is not provoking any conformational changes of the photochromic molecules.

Notably, similar experiments were conducted on 1L-MoS₂-mSAM and 1L-MoS₂-mSAM-Cl. Fig. 2(a) shows the normalised integrated PL spectra when the HS-C₆AZO are in *trans* for excitation powers $P_0 = 1.23$ W/mm², $P_1 = 6.13$ W/mm², $P_2 = 47.7$ W/mm², $P_3 = 45$ W/mm², and $P_4 = 1060$ W/mm². At lowest excitation power (P_0), the recorded PL (red spectrum) is asymmetric, showing a main neutral excitonic peak (X_0) at ~ 1.943 eV as well as a broad side-band (D), on the lower energy side. At higher excitation powers, the intensity of the X_0 peak increases linearly, while the D peak slowly saturates. At the excitation power P_2 , the spectrum starts to decrease, while the PL red shifts and the

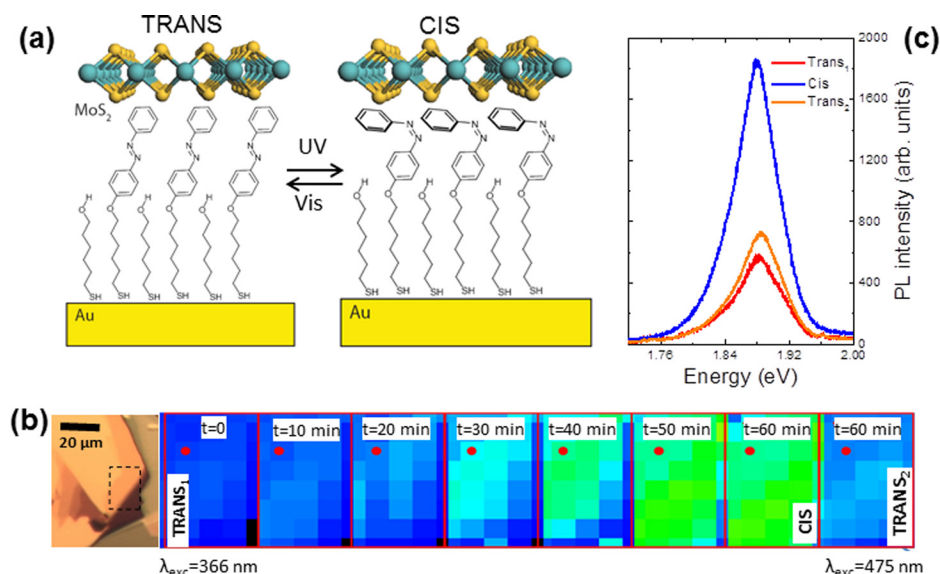


FIG. 1. (a) Schematic image of the sample molecularly gated in *trans* and in *cis*. (b) Series of the PL intensity recorded from the MoS₂-mSAM for 2L-MoS₂ after UV exposure, irradiating the sample for different times ($t = 0$, $t = 10$ min, $t = 20$ min, $t = 30$ min, $t = 40$ min, $t = 50$ min, and $t = 60$ min) at the position of the red spot. Last panel shows the switching back in *trans* after 120 min of white light exposure. (c) PL spectra recorded from the 2L-MoS₂ in *trans* (red spectrum) in *cis* (blue spectrum) and again in *trans* (orange spectrum).

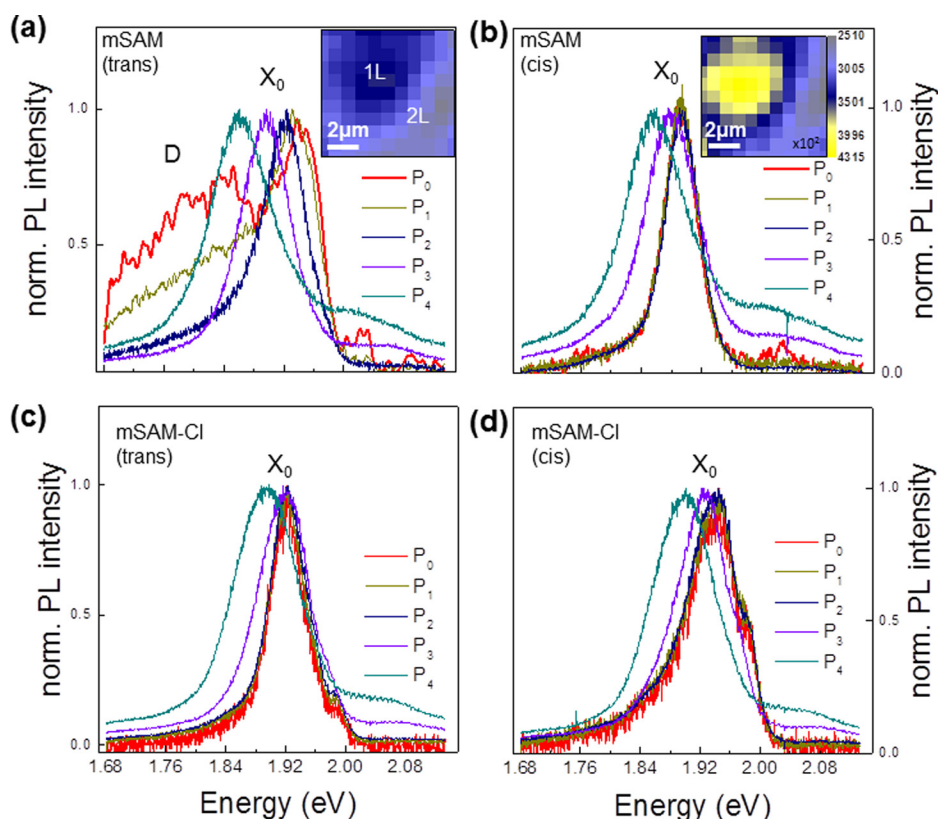


FIG. 2. (a) Normalised power dependence PL spectra recorded from the 1L-MoS₂-mSAM in *trans* and in (b) *cis* with an excitation power from $P_0 = 1.23 \text{ W/mm}^2$ up to $P_4 = 1060 \text{ W/mm}^2$. The inset shows the integrated PL map intensity of the MoS₂-mSAM with the HS-C₆AZO. (c) Normalised power dependent PL spectra recorded from the 1L-MoS₂-mSAM-Cl in *trans* and in (d) in *cis* for excitation powers $P_0 = 1.23 \text{ W/mm}^2$ up to $P_4 = 1060 \text{ W/mm}^2$.

FWHM becomes broader. Similarly, in *cis* (Fig. 2(b)) the PL spectrum ($\sim 1.894 \text{ eV}$; P_0) is red shifted with the excitation power and the FWHM increases. However, the D-peak is now completely suppressed. Both measurements, performed in *trans* and in *cis*, show a clear red-shift of the spectra as the laser power is enhanced and also the FWHM increases. The size of the red-shift differs between the *trans* and the *cis* configuration, being $\Delta_{1T} = 80 \text{ meV}$ in *trans* and $\Delta_{1C} = 40 \text{ meV}$ in *cis*.

We now consider the results obtained using mSAM-Cl (Figs. 2(c)–2(d)). Here, the PL spectra recorded either in *trans* or in *cis* shows no D-peak and the PL intensity shows opposite behaviour compared to the sample with the mSAM discussed above. At low excitation powers, the PL spectra are symmetric at $\sim 1.92 \text{ eV}$ in *trans* (Fig. 2(c)) and asymmetric in *cis* with a maximum at $\sim 1.945 \text{ eV}$ and a feature on the higher energy side of the PL spectrum at $\sim 1.98 \text{ eV}$ (Fig. 2(d)). By increasing the excitation power, the PL spectra get broader and red-shift by about $\Delta_{2T} = 24 \text{ meV}$ in *trans* and of $\Delta_{2C} = 40 \text{ meV}$ in *cis*. Notice that the red-shift upon increasing the excitation power is higher in *cis* than in *trans* for the sample MoS₂-mSAM-Cl, in contrast to MoS₂-mSAM, where the observed red-shift in *trans* is almost twice as that for *cis*.

The unexpected red-shift of the PL spectra dependent on excitation power, observed for both the two types of samples (1L-MoS₂-mSAM and 1L-MoS₂-mSAM-Cl), cannot be attributed to molecular switching induced by the laser, because there is a reversible PL behaviour anytime we increase and reduce the laser power. Therefore, we exclude any correlation with the molecules. Furthermore, the switching of the molecules from *trans* to *cis* shows a clear PL intensity enhancement as reported in the

respective integrated PL intensity maps in the inset of Figs. 2(a) and 2(b).

Another possible reason of the red-shift and broadening of the spectra upon increasing the excitation power can be attributed to heating. In order to find the cause of this effect, we need to compare these results with reference samples. Indeed, changing the substrate, using SiO₂ instead of quartz, the increase of the excitation power up to $P_4 = 1060 \text{ W/mm}^2$ does not lead to red-shift as neither to broadening or quenching of the PL emission. The main difference in using the two substrates, SiO₂ or quartz, lies on the formation of Au grains with size of $30 \pm 10 \text{ nm}$ in diameter and $4 \pm 1 \text{ nm}$ in height, obtained evaporating Au on the quartz substrate.²⁸ Therefore, we attribute this universal red-shift and the PL intensity decrease upon increasing the excitation power to excitation of localized surface plasmons at grain boundaries. The enhancement or the quenching of the PL emission of the active material can be dictated by the distance between the active material and the metal grains,^{13,29} which is usually optimal at 10 nm for PL enhancement.^{13,30,31} On the other hand, an additional recognized plasmonic effect is the PL red-shift when the emitter and the metal grains are too close (below 10 nm), which can be explained as a dipole-dipole interaction between the emitter and the metal grain.^{31,32}

PL spectra recorded from the sample MoS₂-mSAM and MoS₂-mSAM-Cl (red spectra) are presented in Figs. 3(a) and 3(b), showing clearly the impact that the two types of azobenzene molecules have on the 2D crystal. That is a symmetric PL spectrum and $8 \times$ more intensity for the case of HS-C₆AZO-Cl with respect to the HS-C₆AZO, when both types of molecules are in *trans*. Switching the molecules in *cis* (blue spectra) improves the PL signal only for the sample with HS-C₆AZO of about $2.5 \times$ (Fig. 3(a)) and

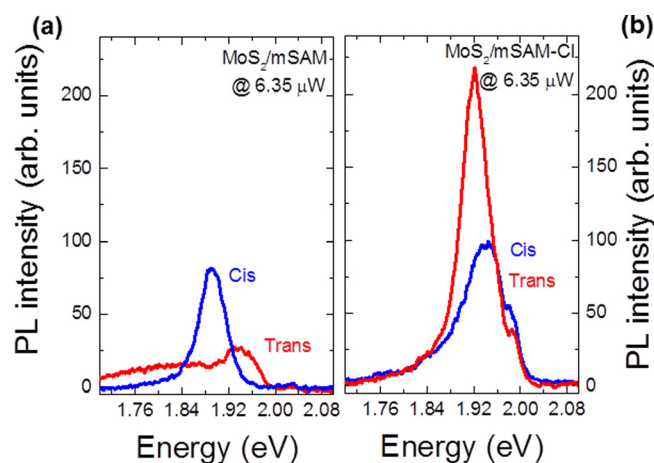


FIG. 3. (a) PL spectra recorded from monolayer MoS₂ on an mSAM on Au-substrate either in *trans* (red) or in *cis* (blue). (b) PL spectra recorded from 1L-MoS₂ on an mSAM-Cl on Au-substrate either in *trans* (red) or in *cis* (blue).

instead, lower the PL of the same amount for the sample with HS-C₆AZO-Cl (Fig. 3(b)). Therefore, by carefully choosing the type of the molecules, one can tune the optical properties of the 2D crystals.

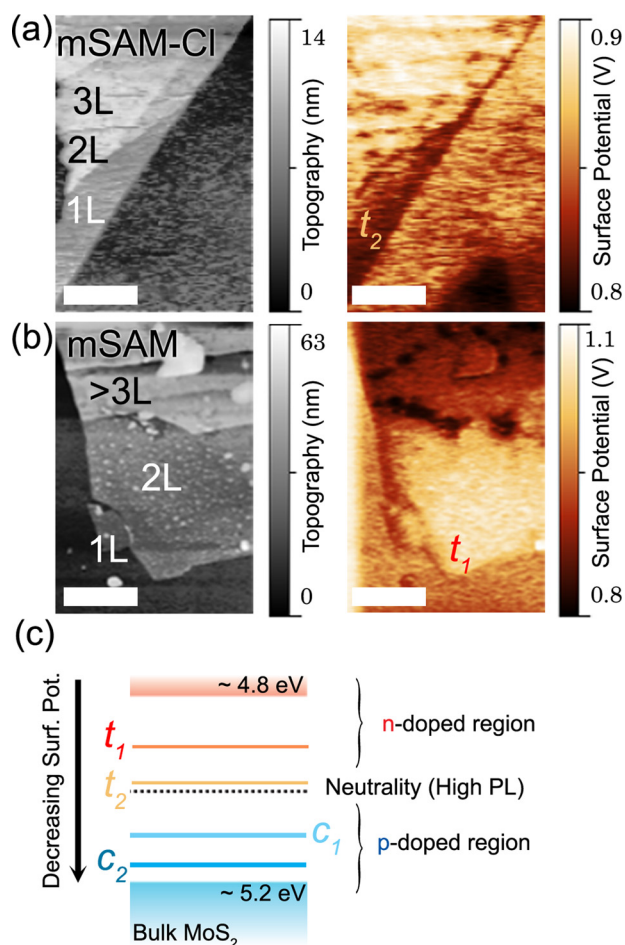


FIG. 4. (a) AFM (left) and KPFM (right) measurements recorded from multilayers MoS₂-mSAM-Cl and (b) from multilayers MoS₂-mSAM samples in *trans*. (c) Energy level diagram showing increased doping when deviating from the bulk MoS₂ charge neutrality. The surface potential of the *cis* *c*₁ and *c*₂ forms is given in the supplementary material.²⁸

In order to understand the reason behind the switchable optical properties as well as the opposite behaviour of the two azobenzene molecules, we performed KPFM measurements for both the two samples MoS₂-mSAM-Au and MoS₂-mSAM-Cl-Au, in *trans* and in *cis*.

Figs. 4(a) and 4(b) show the KPFM measurements of the surface potential (SP) of MoS₂-*trans*-mSAM-Cl and MoS₂-*trans*-mSAM, respectively. The highest SP is found for MoS₂-mSAM hybrids. In absolute terms, an increase of the SP is associated with a lower work function, thus increasing the n-doping character. Likewise, in relative terms, an increase of the SP from multilayer (>3L) MoS₂-mSAM to the 1L-MoS₂-mSAM (Fig. 4(a)) indicates that the Fermi level goes upward, thereby suggesting n-type of doping on the 1L-MoS₂. For MoS₂-mSAM-Cl, the absolute surface potential values are lower and the trend is reversed, indicating a lower doping or even p-doped (Fig. 4(b)). Figure 4(c) qualitatively illustrates these observations.

The observation of a higher n-type doping level for MoS₂-*trans*-mSAM is in agreement with drastic quenching of the integrated PL intensity,¹² as reported in Fig. 3(a) (red spectrum). Accordingly, the PL intensity is higher for *trans*-mSAM-Cl where a lower doping level in *trans* (red spectrum) is present. When the molecules switch in *cis*, the surface potential is strongly shifted to lower values by up to 300 mV.²⁸

Thus, the Fermi energy for both *cis* forms of the molecules shifts the Fermi level towards lower energy, increasing the neutral exciton efficiency (blue spectrum in Fig. 3(a)). It is interesting to note that the sample MoS₂-mSAM-Cl in *trans* has higher PL intensity than the molecules in *cis*. This can be understood as a lower p-doping level in MoS₂-*trans*-mSAM-Cl as compared to the *cis* counterparts. The more asymmetric shape in *cis* compared to *trans*, showing a broadening at ~1.98 eV, can be attributed to an excess of positively charged density that in this case might create positive trions, thereby decreasing the overall PL intensity. Note that our observations extend and complement those by Mauri *et al.*¹² While p-doping does increase the PL yield relative to n-doping, it decreases the PL yield relative to the undoped material.

In conclusion, we presented a study on the optical properties of the MoS₂ mono- and multi-layers exfoliated on top of Au substrate functionalized with azobenzene molecules. An increase of PL emission between *trans*-mSAM and *cis*-mSAM was recorded using a photo-tunable n-type of doping, and opposite behaviour was recorded for the photo-tunable p-type of doping. This was possible using photoswitching azobenzene molecules proximal to MoS₂ monolayer, which tune the Fermi level of the proximal material, tuning the doping between *trans* and *cis*. Through KPFM, we confirm the type of doping induced by the two mixed monolayers mSAM and mSAM-Cl, by looking at the surface potentials both in *trans* and in *cis* for the different layer thicknesses.

We are grateful to DFG for financial support via the NIM and the China scholarship council.

¹J. A. Wilson and A. D. Yoffe, *Adv. Phys.* **18**, 193 (1969).

²L. Mattheiss, *Phys. Rev. B* **8**, 3719 (1973).

³A. Kuc, N. Zibouche, and T. Heine, *Phys. Rev. B* **83**, 245213 (2011).

- ⁴B. Radisavljevic, A. Radenovic, J. Brivio, V. Giacometti, and A. Kis, *Nat. Nanotechnol.* **6**, 147 (2011).
- ⁵Z. Yin, H. Li, H. Li, L. Jiang, Y. Shi, Y. Sun, G. Lu, Q. Zhang, X. Chen, and H. Zhang, *ACS Nano* **6**, 74 (2012).
- ⁶R. S. Sundaram, M. Engel, A. Lombardo, R. Krupke, A. C. Ferrari, P. Avouris, and M. Steiner, *Nano Lett.* **13**, 1416 (2013).
- ⁷J. S. Ross, P. Klement, A. M. Jones, N. J. Ghimire, J. Yan, D. G. Mandrus, T. Taniguchi, K. Watanabe, K. Kitamura, W. Yao, D. H. Cobden, and X. Xu, *Nat. Nanotechnol.* **9**, 268 (2014).
- ⁸H. J. Conley, B. Wang, J. I. Ziegler, R. F. Haglund, S. T. Pantelides, and K. I. Bolotin, *Nano Lett.* **13**, 3626 (2013).
- ⁹K. F. Mak, K. He, C. Lee, G. H. Lee, J. Hone, T. F. Heinz, and J. Shan, *Nat. Mater.* **12**, 207 (2012).
- ¹⁰S. Das, H.-Y. Chen, A. V. Penumatcha, and J. Appenzeller, *Nano Lett.* **13**, 100 (2013).
- ¹¹K. Dolui, I. Rungger, and S. Sanvito, *Phys. Rev. B* **87**, 165402 (2013).
- ¹²S. Mouri, Y. Miyauchi, and K. Matsuda, *Nano Lett.* **13**, 5944 (2013).
- ¹³L. Lu, D. Chen, F. Sun, X. Ren, Z. Han, and G. Guo, *Chem. Phys. Lett.* **492**, 71 (2010).
- ¹⁴J. E. Meinhart, *J. Appl. Phys.* **35**, 3059 (1964).
- ¹⁵N. Crivillers, A. Liscio, F. Di Stasio, C. van Dyck, S. Osella, D. Cornil, S. Mian, G. M. Lazzerini, O. Fenwick, E. Orgiu, F. Reinders, S. Braun, M. Fahlman, M. Mayor, J. Cornil, V. Palermo, F. Cacialli, and P. Samori, *Phys. Chem. Chem. Phys.* **13**, 14302 (2011).
- ¹⁶N. Crivillers, S. Osella, C. van Dyck, G. M. Lazzerini, D. Cornil, A. Liscio, F. Di Stasio, S. Mian, O. Fenwick, F. Reinders, M. Neuburger, E. Treossi, M. Mayor, V. Pale mo, F. Cacialli, J. Cornil, and P. Samori, *Adv. Mater.* **25**, 432 (2013).
- ¹⁷E. Merino and M. Ribagorda, *Beilstein J. Org. Chem.* **8**, 1071 (2012).
- ¹⁸V. Georgakilas, M. Otyepka, A. B. Bourlinos, V. Chandra, N. Kim, K. C. Kemp, P. Hobza, R. Zboril, and K. S. Kim, *Chem. Rev.* **112**, 6156 (2012).
- ¹⁹D. Samanta and A. Sarkar, *Chem. Soc. Rev.* **40**, 2567 (2011).
- ²⁰C. Simão, M. Mas-Torrent, N. Crivillers, V. Lloveras, J. M. Artés, P. Gorostiza, J. Veciana, and C. Rovira, *Nat. Chem.* **3**, 359 (2011).
- ²¹S. A. DiBenedetto, A. Facchetti, M. A. Ratner, and T. J. Marks, *Adv. Mater.* **21**, 1407 (2009).
- ²²E. Margapoti, P. Strobel, M. M. Asmar, M. Seifert, J. Li, M. Sachsenhauser, O. Ceylan, C. A. Palma, J. V. Barth, J. A. Garrido, A. Cattani-Scholz, S. E. Ulloa, and J. Finley, *Nano Lett.* **14**, 6823 (2014).
- ²³M. Buscema, G. A. Steele, H. S. J. van der Zant, and A. Castellanos-Gomez, *Nano Res.* **7**, 1 (2014).
- ²⁴O. Ochedowski, K. Marinov, N. Scheuschner, A. Poloczek, B. K. Bussmann, J. Maultzsch, and M. Schleberger, *Beilstein J. Nanotechnol.* **5**, 291 (2014).
- ²⁵Y. B. Zheng, J. L. Payton, C.-H. Chung, R. Liu, S. Cheunkar, B. K. Pathem, Y. Yang, L. Jensen, and P. S. Weiss, *Nano Lett.* **11**, 3447 (2011).
- ²⁶K. Kreger, P. Wolfer, H. Audorff, L. Kador, N. S. Stutzmann, P. Smith, and H.-W. Schmidt, *J. Am. Chem. Soc.* **132**, 509 (2010).
- ²⁷T. Suzuki, Y. Nagano, A. Kouketsu, A. Matsuura, S. Maruyama, M. Kurotaki, H. Nakagawa, and N. Miyata, *J. Med. Chem.* **48**, 1019 (2005).
- ²⁸See supplementary material at <http://dx.doi.org/10.1063/1.4904824> for Figure S1.
- ²⁹E. Margapoti, D. Gentili, M. Amelia, A. Credi, V. M. Randi, and M. Cavallini, *Nanoscale* **6**, 741 (2014).
- ³⁰O. Kulakovich, N. Strekal, A. Yaroshevich, S. Maskevich, S. Gaponenko, I. Nabiev, U. Woggon, and M. Artemyev, *Nano Lett.* **2**, 1449 (2002).
- ³¹I. M. Soganci, S. Nizamoglu, E. Mutlugun, O. Akin, and H. V. Demir, *Opt. Express* **15**, 14289 (2007).
- ³²V. I. Boev, S. A. Filonovich, M. I. Vasilevskiy, C. J. Silva, M. Gomes, D. V. Talapin, and A. L. Rogach, *Phys. B: Condens. Matter* **338**, 347 (2003).